

Mass-Spectrometric Study on Ion–Molecule Reactions of CF_3^+ with Monosubstituted Benzenes Carrying a Hydroxy or Alkoxy Group at Near-Thermal Energies

Masaharu Tsuji,* Masato Aizawa,† and Yukio Nishimura

Institute of Advanced Material Study, Kyushu University, Kasuga, Fukuoka 816

†Department of Molecular Science and Technology, Graduate School of Engineering Sciences, Kyushu University, Kasuga, Fukuoka 816

(Received July 26, 1995)

The gas-phase ion-molecule reactions of CF_3^+ with monosubstituted benzenes carrying a hydroxy or alkoxy group [PhX: X = OH, CH_2OH , $\text{CH}_2\text{CH}_2\text{OH}$, $\text{CH}(\text{OH})\text{CH}_3$, OCH_3 , and OC_2H_5] have been studied at near-thermal energies using an ion-beam apparatus. The major product channels are electrophilic addition on the O-atom, followed by loss of CF_3OH , for ROH (R = Ph, PhCH_2 , PhCH_2CH_2 , PhCHCH_3); while they are electrophilic addition to a ring and a substituent, followed by molecular eliminations such as HF, C_2H_4 , and PhF, for PhOCH_3 and PhOC_2H_5 . As a minor product channel, charge transfer is found for PhOH, PhOCH_3 , and PhOC_2H_5 . The reaction mechanism is discussed based on product ion distributions and theoretical calculations of the potential energies of reaction pathways.

We have recently initiated systematic mass spectrometric studies on ion-molecule reactions of a typical superacid, CF_3^+ , with aromatic molecules in order to clarify the reactivity of carbocations for aromatic molecules in the gas phase completely free from any solvent. In preceding papers,^{1–4} product ion distributions have been reported for PhX [X = H, CH_3 , C_2H_n ($n = 1, 3, 5$), NH_2 , NO_2 , CN, and OCH_3]. The reactions of CF_3^+ with the above monosubstituted benzenes generate product channels as follows: (1) an electrophilic attack on a ring without highly reactive substituents (e.g. benzene and toluene), (2) an electrophilic attack on a substituent with lone-pair electrons and multiple bonds (e.g. anisole and benzonitrile), and (3) an attack on a negative charge (nitrobenzene). On the basis of our previous results, we expected that preferential σ -bond formation by trifluoromethylation would occur at polarizable centers of negative charge (i.e. lone-pair electrons and multiple bonds) in the gas-phase where polar heteroatoms are not solvated. The charge-transfer (CT) process was found to compete with the above main reactions for almost all monosubstituted benzenes with ionization potentials (IP) lower than the recombination energy of CF_3^+ (≤ 8.90 eV), which is equal to the IP of $\text{CF}_3\cdot$. The branching ratio of the CT channel increases with decreasing the IP of the reagents. For aniline with the lowest ionization potential, the CT process becomes a dominant product channel ($71.7 \pm 0.5\%$). Although the hydride-transfer (HT) process was found for such aromatic hydrocarbons as benzene and toluene, it was absent for PhNH_2 , PhNO_2 , PhCN , and PhOCH_3 which have highly reactive substituents.

In the present work, ion-molecule reactions of CF_3^+ with PhX [X = OH, CH_2OH , $\text{CH}_2\text{CH}_2\text{OH}$, $\text{CH}(\text{OH})\text{CH}_3$, OCH_3 ,

and OC_2H_5] were studied in order to examine the effects of a hydroxy or alkoxy group in the monosubstituted benzenes. All of these reagents have highly reactive lone-pair electrons on the oxygen atom. Therefore, not only the electrophilic addition to a benzene ring but also that to a substituent is possible. The reaction mechanism is discussed based on product ion distributions and semiempirical calculations of potential energies of reaction pathways. The results obtained are compared with previous studies on the reactions of CF_3^+ with aliphatic alcohols by using an ion-cyclotron resonance (ICR) method.^{6,7} Although the product ion distribution for PhOCH_3 has been reported in our recent report,² no theoretical calculations of the reaction pathways have been carried out. In the present study, potential energies are calculated semiempirically in order to confirm the validity of the reaction scheme proposed previously.

Experimental

The ion-beam apparatus used in the present study was identical with that reported previously.^{1–4} In brief, ground-state $\text{Ar}^+(\text{P}_{3/2})$ ions were generated by a microwave discharge of high-purity Ar gas in a quartz flow tube. The reactant CF_3^+ ions were produced by the thermal-energy CT reaction of Ar^+ with CF_4 .¹ They were expanded into a low-pressure chamber through a nozzle centered on the flow tube. The reagent gas was injected into the reaction zone from an orifice placed 5 cm downstream from the nozzle. The reactant and product ions were sampled through an orifice placed 3 cm further downstream, and were analyzed using a quadrupole mass spectrometer. The operating pressures were 0.5–1.0 Torr (1 Torr = 133.322 Pa) in the ion-source chamber, $(1.5\text{--}2.5) \times 10^{-3}$ Torr in the reaction chamber, and $(0.8\text{--}2.0) \times 10^{-5}$ Torr in the mass analyzing chamber. The partial pressures of the sample gases were

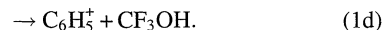
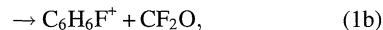
$< 1 \times 10^{-5}$ Torr in the reaction chamber and $< 1 \times 10^{-6}$ Torr in the mass-analyzing chamber.

Under a typical Ar pressure in the flow tube (1.0 Torr), the Ar expansion was estimated from known relations⁵⁾ to have a Mach number of 3.2 and a final velocity of 487 m s^{-1} . Assuming a Boltzmann distribution of 300 K for reagent molecules and a perpendicular direction between the ion-beam and the reagent, the relative velocities of the CF_3^+ -PhOH, CF_3^+ -PhOC₂H₅, CF_3^+ -PhCH₂OH, CF_3^+ -PhCH₂CH₂OH, and CF_3^+ -PhCH(OH)CH₃ pairs were evaluated to be 552, 538, 544, 538, and 538 m s^{-1} , corresponding to average center-of-mass translational energies of 63, 66, 65, 66, and 66 meV, respectively. Therefore, the present experiments were carried out at only slightly hyperthermal energies. The reaction time between CF_3^+ and the reagents was estimated to be $< 5 \times 10^{-5} \text{ s}$ by using the velocity of the CF_3^+ beam and the distance between the reagent gas inlet and the sampling orifice. In the present experiment, the sample gas pressures were too low to control by using a mass flowmeter. Therefore, it was difficult to determine the reaction rate coefficients.

The heats of formation are known for the reactant ion, reagents, and some stable products obtained in this work.^{8,9)} However, there are many species whose ΔH° values are unknown. They were calculated by using a semiempirical MNDO method (MOPAC Ver. 6.0) in order to describe potential-energy diagrams of the reaction pathways. The IP values of PhCH₂CH₂OH and PhCH(OH)CH₃ were calculated by using not only the MNDO method but also AM1 and PM3 methods.

Results and Discussion

Phenol: For the CF_3^+ + PhOH reaction, the following four product channels were observed:



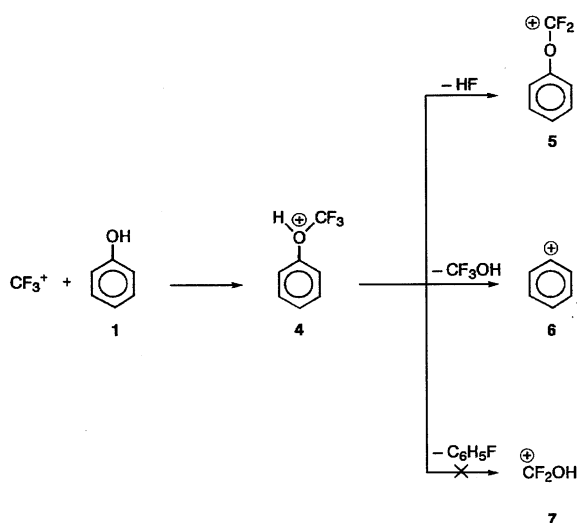
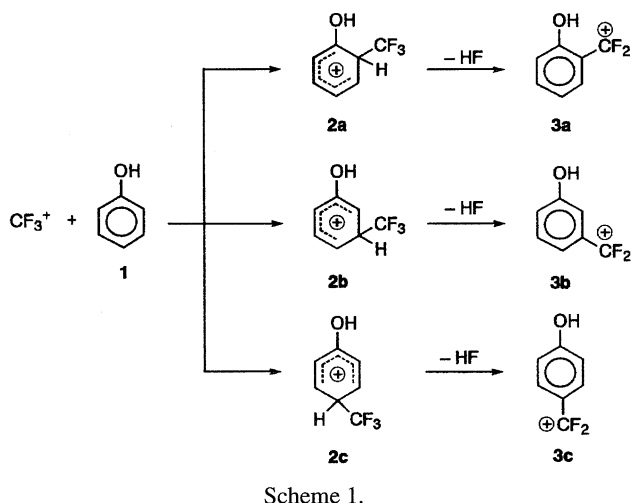
The branching ratios of each process are given in Table 1. Major product channels are electrophilic addition with a loss of HF or CF_3OH , Eqs. 1a and 1d, which occupy about 90% of the total ion production. As minor product channels, electrophilic addition followed by CF_2O elimination and CT leading to the parent ion, Eqs. 1b and 1c, were observed with the same branching ratios of about 5%. Although the initial adduct $\text{C}_8\text{H}_8\text{OF}_3^+$ ion was observed for the reaction with PhOCH₃ ($15.4 \pm 2.4\%$),²⁾ the corresponding adduct $\text{C}_7\text{H}_6\text{OF}_3^+$ ion could not be detected for PhOH.

The $\text{C}_7\text{H}_5\text{OF}_2^+$ ion can be formed through the ring and substituent adducts (Schemes 1 and 2). The electron-donating resonance effect of the OH group will enhance the formation of Wheland-type adducts (**2a**—**2c**), while a high reactivity of the lone-pair electrons on the oxygen atom will yield O-adduct **4**, preferentially. The potential-energy diagram for

Table 1. Product Ion Distributions and Reaction Mechanism in Ion-Molecule Reactions of CF_3^+ with $\text{C}_6\text{H}_5\text{OH}$, $\text{C}_6\text{H}_5\text{C}_m\text{H}_{2m}\text{OH}$ ($m = 1, 2$), and $\text{C}_6\text{H}_5\text{OC}_m\text{H}_{2m+1}$ ($m = 1, 2$), at Near-Thermal Energy^{a)}

Reagent	Product ion	Reaction mechanism	Branching ratio/%
$\text{C}_6\text{H}_5\text{OH}$	$\text{C}_7\text{H}_5\text{OF}_2^+$	EA ^{b)}	37.1 ± 1.8
	$\text{C}_6\text{H}_6\text{F}^+$	EA	4.9 ± 1.2
	$(\text{C}_6\text{H}_5\text{OH})^{++}$	CT ^{c)}	4.8 ± 1.3
	C_6H_5^+	EA	53.2 ± 1.8
$\text{C}_6\text{H}_5\text{CH}_2\text{OH}$	$\text{C}_7\text{H}_5\text{OF}_2^+$	EA	32.6 ± 2.9
	$(\text{C}_6\text{H}_5\text{CH}_2)^+$	EA	67.4 ± 2.9
$\text{C}_6\text{H}_5\text{CH}_2\text{CH}_2\text{OH}$	$(\text{C}_6\text{H}_5\text{CH}_2\text{CH}_2)^+$	EA	60.2 ± 2.9
	$(\text{C}_6\text{H}_5\text{CH}_2)^+$	EA	14.6 ± 0.7
	$(\text{CH}_2\text{CH}_2\text{OH})^+$	EA	25.2 ± 2.5
	$(\text{C}_6\text{H}_5\text{CHCH}_3)^+$	EA	64.0 ± 2.2
$\text{C}_6\text{H}_5\text{CH(OH)CH}_3$	$[\text{CH(OH)CH}_3]^+$	EA	36.0 ± 2.2
	$\text{C}_8\text{H}_8\text{OF}_3^+$	EA	15.4 ± 2.4
$\text{C}_6\text{H}_5\text{OCH}_3$	$\text{C}_8\text{H}_7\text{OF}_2^+$	EA	35.7 ± 4.3
	$(\text{C}_6\text{H}_5\text{OCH}_3)^{++}$	CT	14.4 ± 1.8
	C_6H_5^+	EA	16.7 ± 3.0
	$(\text{CH}_3\text{OCF}_2)^+$	EA	17.8 ± 2.7
	$\text{C}_7\text{H}_6\text{OF}_3^+$	EA	42.9 ± 3.2
$\text{C}_6\text{H}_5\text{OC}_2\text{H}_5$	$\text{C}_7\text{H}_5\text{OF}_2^+$	EA	28.0 ± 1.4
	$(\text{C}_6\text{H}_5\text{OC}_2\text{H}_5)^{++}$	CT	11.9 ± 1.2
	$\text{C}_6\text{H}_6\text{F}^+$	EA	2.3 ± 0.2
	$(\text{C}_2\text{H}_5\text{OCF}_2)^+$	EA	2.9 ± 0.2
	$\text{C}_6\text{H}_6\text{O}^{++}$	CT	3.5 ± 0.2
	C_6H_5^+	EA	4.4 ± 1.2
	C_2H_5^+	EA	4.1 ± 0.4

a) Data for $\text{C}_6\text{H}_5\text{OCH}_3$ are obtained from Ref. 2. b) Electrophilic addition. c) Charge transfer.



the two CF_3^+ -addition/HF-elimination pathways were evaluated from reported thermochemical data⁹⁾ of CF_3^+ , PhOH, and HF and calculated ΔH° values of four $\text{C}_7\text{H}_6\text{OF}_3^+$ and $\text{C}_7\text{H}_5\text{OF}_2^+$ ions. The results obtained are shown in Fig. 1. The ΔH° values of ring adducts **2a**–**2c** and O-adduct **4** are higher than those of **3a**–**3c**+HF and **5**+HF, respectively. Therefore, the adduct ions will completely decompose into $\text{C}_7\text{H}_5\text{OF}_2^+$ +HF, which is consistent with the lack of the initial adduct ion. Although there will be no energy barrier for the formation of the initial adduct ions, high energy barriers will exist in the elimination pathways of HF from the adduct ions. On the basis of these facts, the relative formation rates of the initial adduct ions are governed thermochemically, whereas the relative decomposition rates of the adduct ions are controlled kinetically. Since the ΔH° values of **2a** and **2c** are lower than those of **2b** and **4**, the formation of the former adduct ions is more favorable. According to a recent ab initio calculation of the potential energies of the CF_3^+ + CH_3OH → $\text{CH}_3\text{OCF}_2^+$ +HF pathway,⁷⁾ the energy barrier was estimated to be ca. 1.6 eV. The energy barrier between **4** and **5** may be similar to that of the HF elimination

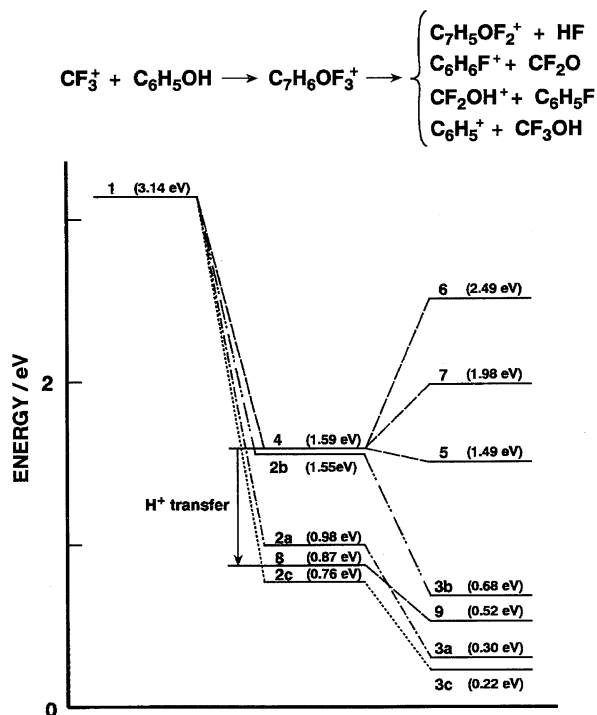
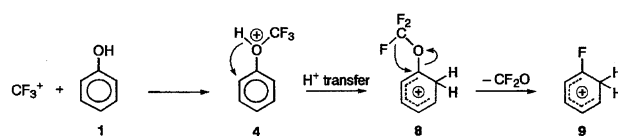


Fig. 1. A potential-energy diagram for the electrophilic CF_3^+ -addition/dissociation pathways in the CF_3^+ +PhOH system.

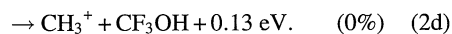
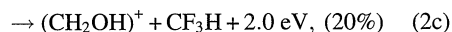
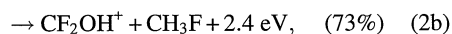
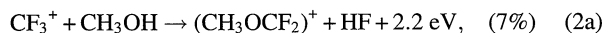
pathway from the oxonium ion formed in the CF_3^+ /PhOH reaction. Unfortunately, no theoretical information about the energy barrier for the HF elimination from the ring adduct ions has been obtained. In order to determine the relative importance of the two CF_3^+ -addition/HF-elimination pathways, further theoretical calculations of activation barriers and an isotopic study are required.

The most probable reaction pathway for the formation of $\text{C}_6\text{H}_6\text{F}^+$ is shown in Scheme 3. The cation **9** is formed through H^+ transfer from **4** to **8**, followed by the elimination of CF_2O . The elimination of CF_2O has often been observed in the reactions of CF_3^+ with such carbonyl compounds as CH_3COCH_3 and $\text{CH}_3\text{COC}_2\text{H}_5$.¹⁰⁾ The C_6H_5^+ ion is exclusively formed through the Ph–O bond cleavage in O-adduct **4** (Scheme 2). The potential-energy diagram for the formation of $\text{C}_6\text{H}_6\text{F}^+$ and C_6H_5^+ is shown in Fig. 1. It should be noted that the ΔH° value of **6**+ CF_3OH is higher than that of **4** by 0.90 eV. This implies that precursor oxonium ion **4** must possess at least an excess internal energy of 0.90 eV before its decomposition into **6**+ CF_3OH .

In a recent ICR experiment of Grandinetti et al.,⁶⁾ three product channels (2a)–(2c) have been found in the CF_3^+ / CH_3OH reaction:



Scheme 3.



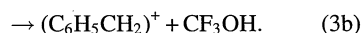
The electrophilic addition to the lone-pair electrons on the oxygen atom, followed by the CH_3F elimination, was the dominant product channel. The addition followed by the CF_3OH elimination, Eq. 2d, was not found, even though it is energetically allowed. For the reaction with PhOH , the former pathway is absent, while the latter one is the most favorable channel, indicating that there is a significant difference in the favorable electrophilic-addition/dissociation-processes between PhOH and CH_3OH .

If the most favorable product channel for PhOH is the same as that for CH_3OH , the formation of **7** via O-adduct **4** is expected (Scheme 2). In order to explain the lack of **7**, the potential energy of **7**+ $\text{C}_6\text{H}_5\text{F}$ is calculated (Fig. 1). Since the ΔH° value of **7**+ $\text{C}_6\text{H}_5\text{F}$ is lower than that of **6**+ CF_3OH , the formation of **7** is more favorable on the basis of the thermochemical stability of the final products. This is inconsistent with the experimental observation. Phenyl cation **6** can be formed by the simple unimolecular decomposition of oxonium ion **4** without an energy barrier. On the other hand, a high energy barrier will exist in the reaction pathway between **4** and **7** because the attack of F^- on the 1-position sp^2 carbon of the bulky phenyl group is unfavorable. This will be a major reason for the lack of **7**. The above finding led us to conclude that the dissociation pathways of oxonium ion **4** are kinetically controlled.

For the reaction with CH_3OH , a loss of CF_3H due to HT from methyl group or 1,2-elimination of the oxonium intermediate, Eq. 2c, was observed as a minor product channel. However, the HT channel could not be detected for PhOH . Taking account of the resonance form of phenol, we think that a negative charge is developed in the benzene ring due to the electron-donating resonance effect of the hydroxy group. This, along with the occurrence of fast competitive electrophilic addition to the ring and the substituent, makes it difficult to abstract H^- from the benzene ring of phenol.

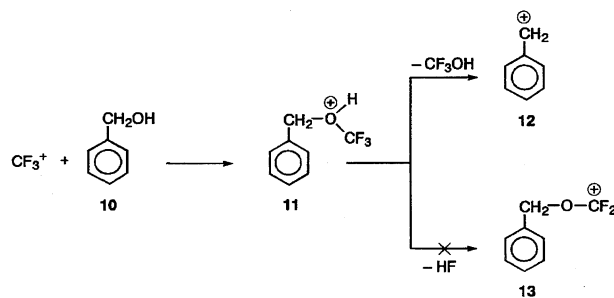
Benzyl, 1-Phenylethyl, and 2-Phenylethyl Alcohols:

For the reaction with PhCH_2OH , only two product channels were observed, with the branching ratios given in Table 1:

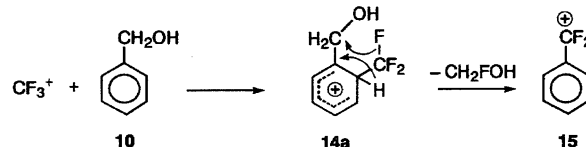


The most favored pathway (3b) proceeds through the simple dissociation of the C–O bond in O-adduct **11** (Scheme 4), indicating that the major product channel is the same for PhCH_2OH and for PhOH . Process (3a), which is absent for PhOH , probably occurs through fluoride-ion and proton transfers from *ortho*-ring adduct **14a** (Scheme 5).

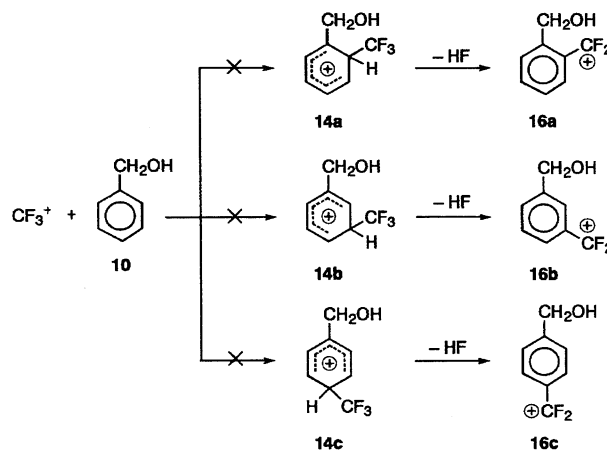
In the case of PhOH , electrophilic addition to the ring and/or the substituent followed by HF elimination occurs. The corresponding processes, shown in Schemes 6 and 4,



Scheme 4.



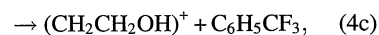
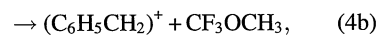
Scheme 5.

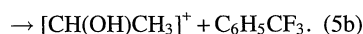
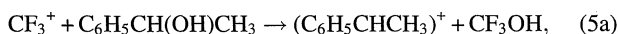


Scheme 6.

could not be found for PhCH_2OH . The potential energies of the electrophilic CF_3^+ -addition/HF-elimination processes are shown in Fig. 2. The HF-elimination is energetically possible from both ring adducts **14a**–**14c** and substituent adduct **11**. It should be noted that the potential energy of the kinetically prevailing **12**+ CF_3OH pathway is lower than those of the CF_3^+ -addition/HF-elimination processes. Although the electron-donating resonance effect enhances the electrophilic addition to the ring, such an effect is blocked by an insertion of the CH_2 group between the Ph and OH groups. The above reasons will result in the disappearance of the addition/HF-elimination processes and the significant enhancement of the formation of **12**.

The following product channels were found for the $\text{CF}_3^+/\text{PhCH}_2\text{CH}_2\text{OH}$ and $\text{CF}_3^+/\text{PhCH}(\text{OH})\text{CH}_3$ reactions, with the branching ratios given in Table 1:





The most probable reaction mechanisms of the above processes are shown in Schemes 7, 8, 9, and 10. The major product channels for the above two alcohols are electrophilic addition to the lone-pair electrons of the O-atom followed by loss of CF_3OH , as in the cases of phenol and benzyl alcohol. It was therefore concluded that the elimination of CF_3OH from oxonium intermediates is the most favorable product channel for monosubstituted benzenes carrying a hydroxy group. As competitive exit channels, losses of CF_3OCH_3 and PhCF_3 from substituent adduct **18** and *ipso*-adduct **21d** via Schemes 7 and 8, respectively, were found for $\text{PhCH}_2\text{CH}_2\text{OH}$, while a loss of PhCF_3 from *ipso*-adduct

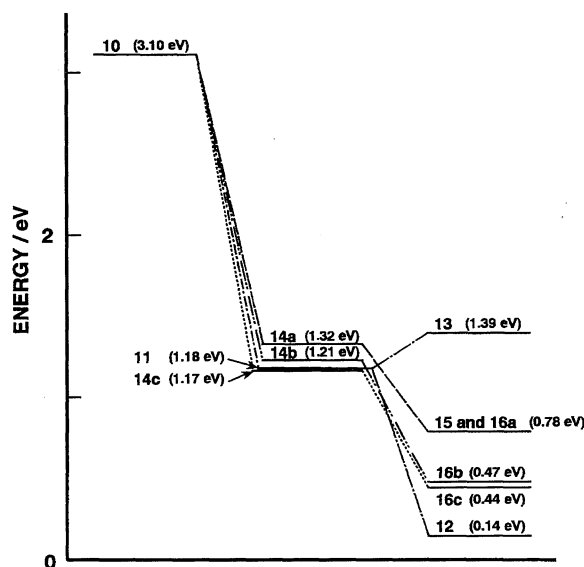
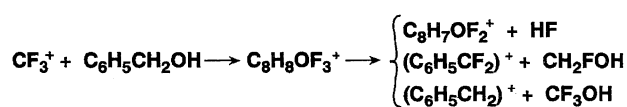
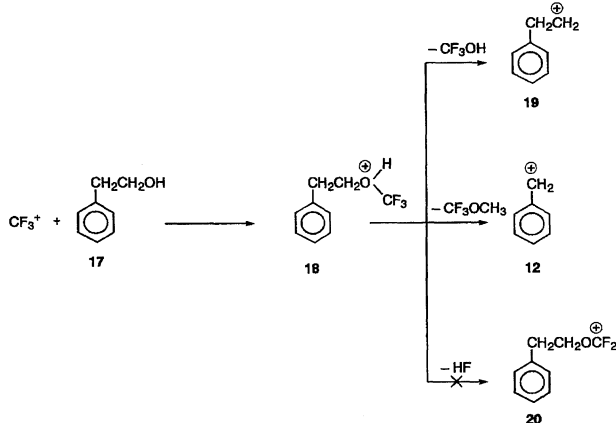


Fig. 2. A potential-energy diagram for the electrophilic CF_3^+ -addition/dissociation pathways in the $\text{CF}_3^+ + \text{PhCH}_2\text{OH}$ system.



Scheme 7.

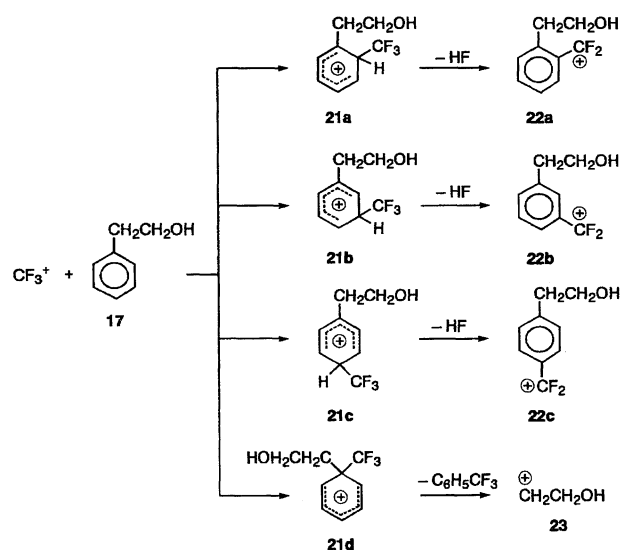
28d via Scheme 10 was observed for $\text{PhCH}(\text{OH})\text{CH}_3$.

Grandinetti et al.⁶⁾ have found only a loss of CF_3OH from the oxonium intermediate in the $\text{CF}_3^+/\text{CH}_3\text{CH}_2\text{OH}$ reaction:

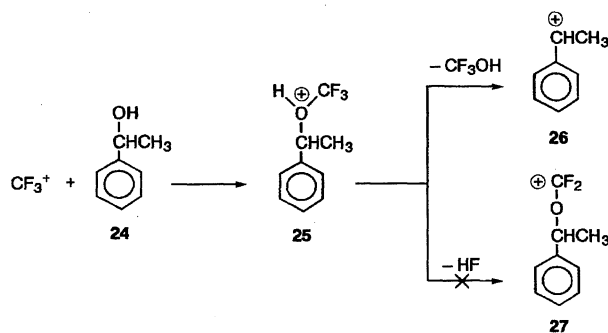


They discussed the reactivity of CF_3^+ toward aliphatic alcohols ROH ($\text{R}=\text{CH}_3, \text{CH}_3\text{CH}_2$) by an interaction between the energy developed between CF_3^+ and n-center of the substrate and the activation barrier for the fragmentation of the encounter complex. The kinetically favorable fragmentation pathways proceed through O-R unimolecular cleavage, leading to $[\text{R}^+\cdot\text{CF}_3\text{OH}]$ fragmentation complex. For $\text{R}=\text{CH}_3$, a rapid fluoride-ion transfer from C to R occurs prior to collapse to products. The same process does not take place for $\text{R}=\text{CH}_3\text{CH}_2$, because it is thermochemically unfavorable with respect to simple dissociation of the complex to R^+ and CF_3OH . We have found here that the dominant pathways in the $\text{CF}_3^+/\text{PhCH}_2\text{CH}_2\text{OH}$ and $\text{CF}_3^+/\text{PhCH}(\text{OH})\text{CH}_3$ reactions are similar to that in the $\text{CF}_3^+/\text{CH}_3\text{CH}_2\text{OH}$ reaction. The lack of fluoride-ion transfer from C to R for $\text{PhCH}_2\text{CH}_2\text{OH}$ and $\text{PhCH}(\text{OH})\text{CH}_3$ will also be due to thermochemical instability in comparison with simple dissociation processes of the oxonium intermediates.

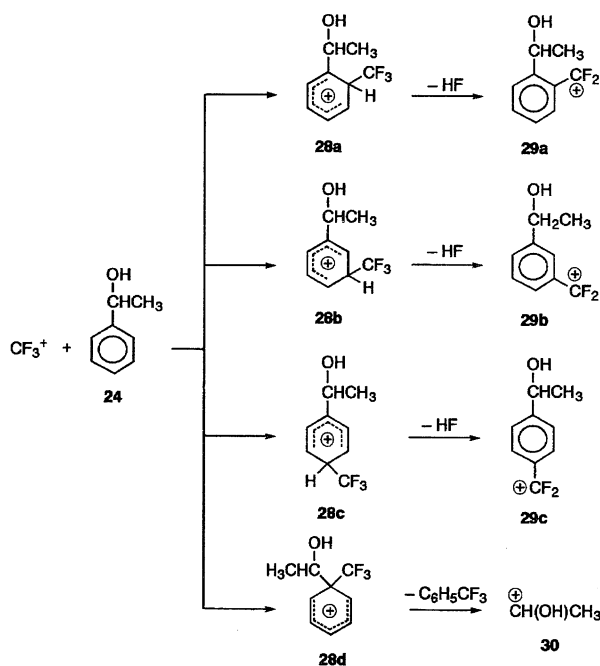
In addition to processes (4a)–(4c) and (5a)–(5b), elec-



Scheme 8.

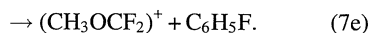
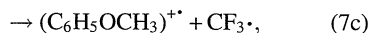
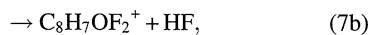
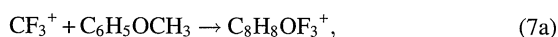


Scheme 9.



trophilic addition to ring and substituent followed by HF elimination can occur via reaction mechanisms shown in Schemes 7, 8, 9, and 10. The potential energies of such processes are shown in Figs. 3 and 4. Although both the ring and substituent CF_3^+ -addition/HF-elimination pathways are energetically accessible, the potential energy of the kinetically favored substituent CF_3^+ -addition/ CF_3OH -dissociation pathway is either comparable with or lower than those of the CF_3^+ -addition/HF-elimination processes for $\text{PhCH}_2\text{CH}_2\text{OH}$ and $\text{PhCH}(\text{OH})\text{CH}_3$. Thus, the lack of the CF_3^+ -addition/HF-elimination processes can be attributed to the occurrence of competitive kinetically prevailing pathways.

Anisole and Phenetole: In our previous study, the following five product channels have been found for PhOCH_3 :



The branching ratios of the above product channels are given in Table 1. The possible reaction mechanisms of Eqs. 7a, 7b, 7d, and 7e are shown in Schemes 11 and 12. The most outstanding feature for the reaction with PhOCH_3 is the appearance of the initial adduct $\text{C}_8\text{H}_8\text{OF}_3^+$ ion. We have recently found that the initial ring adduct $\text{C}_7\text{H}_6\text{F}_3^+$ ion, formed in the $\text{CF}_3^+/\text{C}_6\text{H}_6$ reaction, decomposes completely by loss of HF .^{1,4)} It is highly likely that the ring-adduct $\text{C}_8\text{H}_8\text{OF}_3^+$ ion, formed in the $\text{CF}_3^+/\text{PhOCH}_3$ reaction, also decomposes completely. Therefore, the initial adduct ion has been predicted to be substituent adduct **34**. In order to examine the

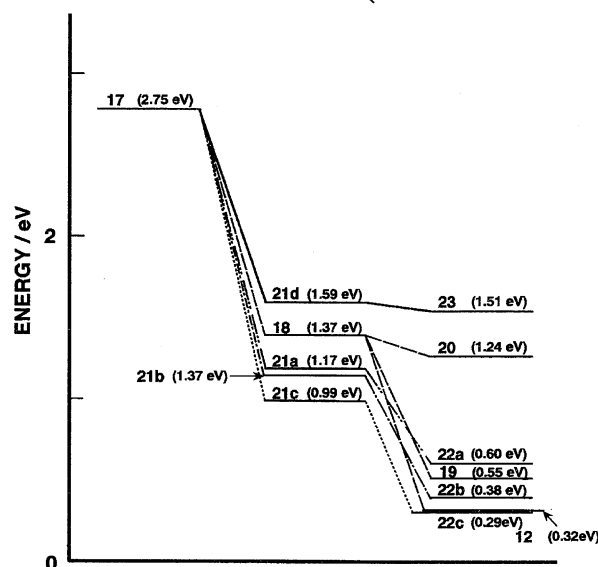
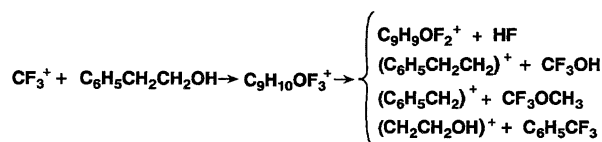


Fig. 3. A potential-energy diagram for the electrophilic CF_3^+ -addition/dissociation pathways in the $\text{CF}_3^+ + \text{PhCH}_2\text{CH}_2\text{OH}$ system.

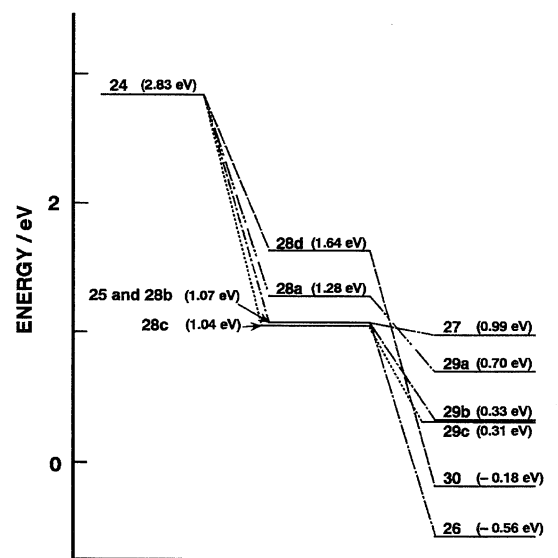
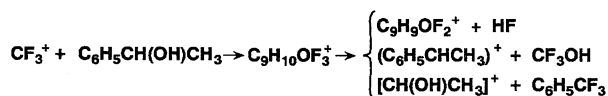
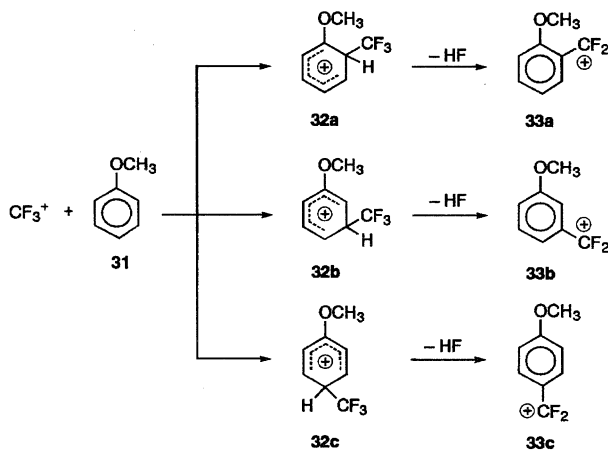
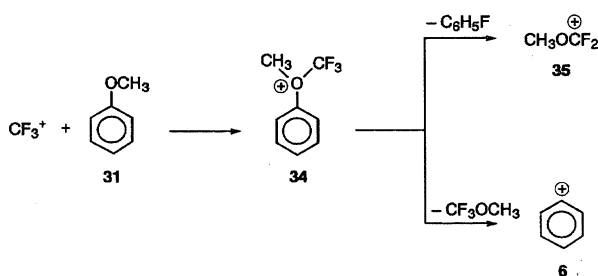


Fig. 4. A potential-energy diagram for the electrophilic CF_3^+ -addition/dissociation pathways in the $\text{CF}_3^+ + \text{PhCH}(\text{OH})\text{CH}_3$ system.

validity of this prediction, the potential energy of the CF_3^+ -addition/HF-elimination pathways was evaluated (Fig. 5). The ΔH° values of initial adduct ions (**32a**—**32c**) are higher than those of **33a**—**33c**+HF. Therefore, the elimination of HF from **32a**—**32c** will occur completely, which supports



Scheme 11.



Scheme 12.

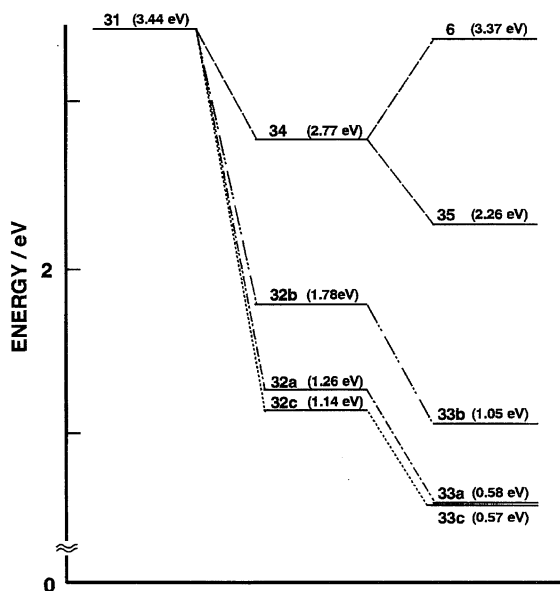
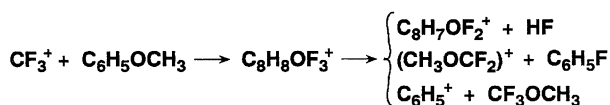
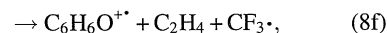
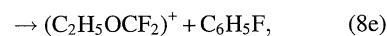
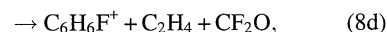
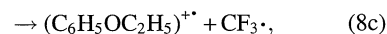
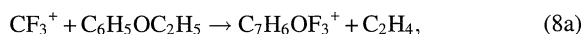


Fig. 5. A potential-energy diagram for the electrophilic CF_3^+ -addition/dissociation pathways in the $\text{CF}_3^+ + \text{PhOCH}_3$ system.

our previous prediction. Although the ΔH° value of $35 + \text{PhF}$ is also lower than 34, initial adduct ion 34 is found. There will be a high energy barrier for the formation of 35 from

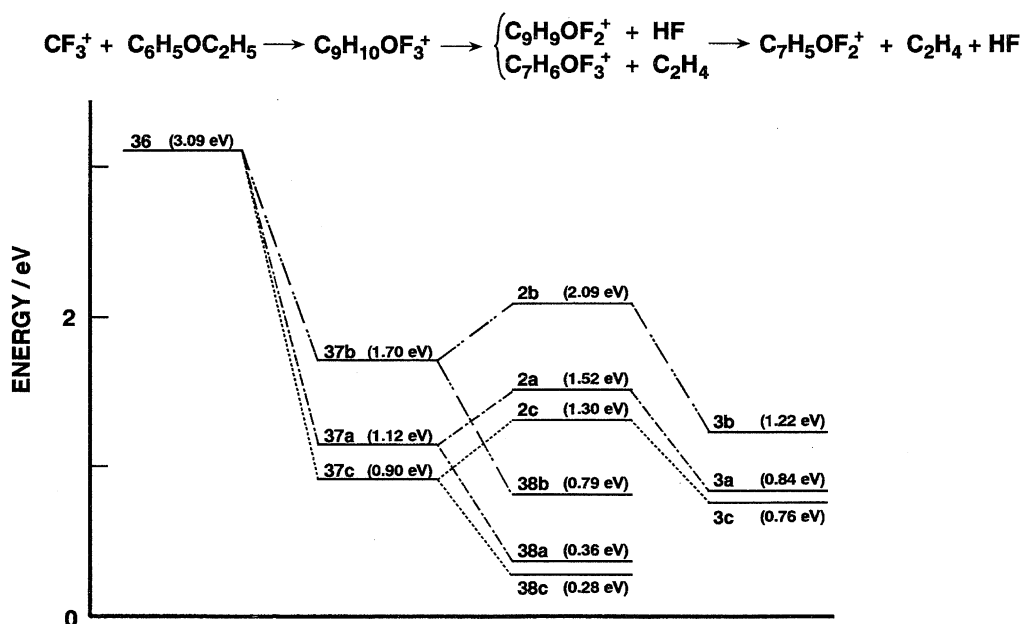
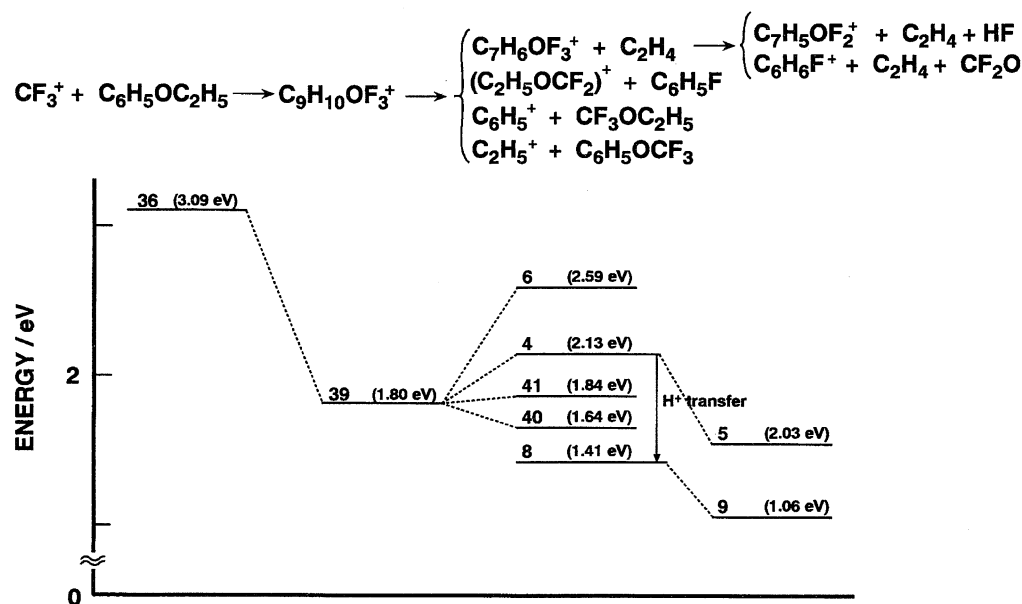
34, because the attack of F^- on 1-position sp^2 carbon of the bulky phenyl group is unfavorable. Therefore, the initial adduct ion 34 will be found from anisole. The radiative associative process, as found for the reactions of NO^+ with such bases as 2-butanone and 3-pentanone¹¹⁾ may take part in the stabilization of 34.

The following eight product channels are observed in the $\text{CF}_3^+ + \text{PhOC}_2\text{H}_5$ reaction, with the branching ratios given in Table 1:



Since the initial adduct ion and the electrophilic CF_3^+ -addition/HF elimination channel could not be found, there exists a significant difference in the product channel between PhOC_2H_5 and PhOCH_3 . The major processes are electrophilic addition followed by C_2H_4 or $\text{C}_2\text{H}_4 + \text{HF}$ elimination, which occupies about 70% of the total ion production. A similar C_2H_4 or $\text{C}_2\text{H}_4 + \text{HF}$ elimination channel was found in the $\text{CF}_3^+/\text{PhC}_2\text{H}_5$ reaction,⁴⁾ indicating that the C_2H_4 -elimination pathways take precedence over the HF-elimination ones for monosubstituted benzenes carrying an ethyl group. The potential-energy diagram of the electrophilic CF_3^+ -addition, followed by various elimination and dissociation processes, is shown in Figs. 6 and 7. The electrophilic addition can occur both on the π electrons of the aromatic ring and lone-pair electrons of the O atom to yield adducts 37a—37c and 39, respectively (Schemes 13 and 14). The formation of the ring adducts is enhanced by the electron-donating resonance effect of the ethoxy group. Since the ring adducts 37a and 37c are more stable than the ring adduct 37b and O-adduct 39, the formation of the former *ortho*- and *para*-adducts will take precedence over that of the latter adducts. Minor processes (8d), (8e), (8g), and (8h) proceed through the decomposition of O-adduct (Scheme 14). The branching ratios of C_6H_5^+ and C_2H_5^+ formed by the simple decomposition of the oxonium ion 39 are larger than those of $\text{C}_6\text{H}_6\text{F}^+$ and $(\text{C}_2\text{H}_5\text{OCF}_2)^+$ which are formed via unstable intermediates. This difference is probably due to the existence of high energy barriers for the formation of the latter ions from 39.

Figure 6 shows the potential-energy diagram of various elimination pathways of HF and C_2H_4 from the ring adducts. The potential energies of HF-elimination pathways are lower than those of the C_2H_4 and $\text{C}_2\text{H}_4 + \text{HF}$ elimination ones. Therefore, most stable ions 38a and 38c will be produced preferentially from 37a and 37c without further elimination

Fig. 6. A potential-energy diagram for the ring-addition/dissociation-pathways in the CF_3^+ + PhOC_2H_5 system.Fig. 7. A potential-energy diagram for the substituent-addition/dissociation pathways in the CF_3^+ + PhOC_2H_5 system.

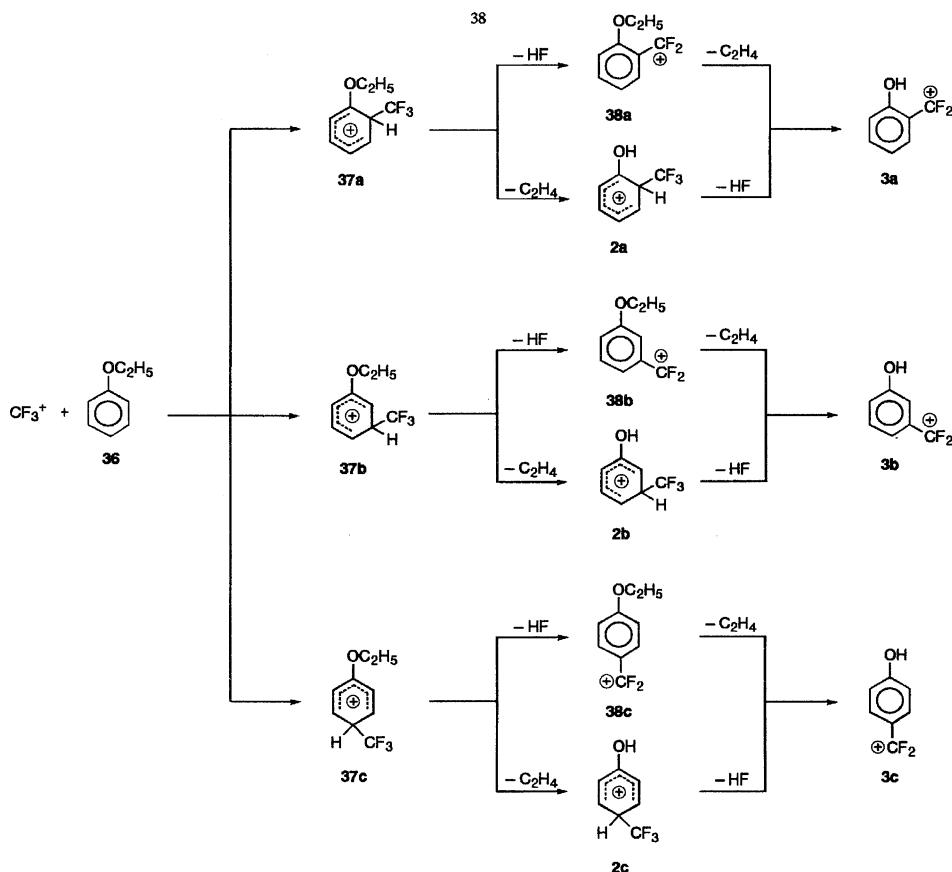
of C_2H_4 , if the elimination of HF occurs at the first step. This is inconsistent with the experimental observation. It was therefore concluded that the elimination of C_2H_4 takes precedence over that of HF, so that the formation of (3a, 3c) takes place via (2a, 2c). The high branching ratios of (2a, 2c) and (3a, 3c) imply that initial adduct ions (37a, 37c) have sufficient internal energy to decompose completely into (2a, 2c) and (3a, 3c).

The CT and dissociative CT processes, (8c) and (8f), are found with a total branching ratio of about 15%. This is the first example where the dissociative CT occurs in the reactions of CF_3^+ with monosubstituted benzenes. The $\text{C}_6\text{H}_6\text{O}^{++}$ ion has been found as the most abundant product ion in the mass spectra under electron-impact ionization.¹²⁾ Two

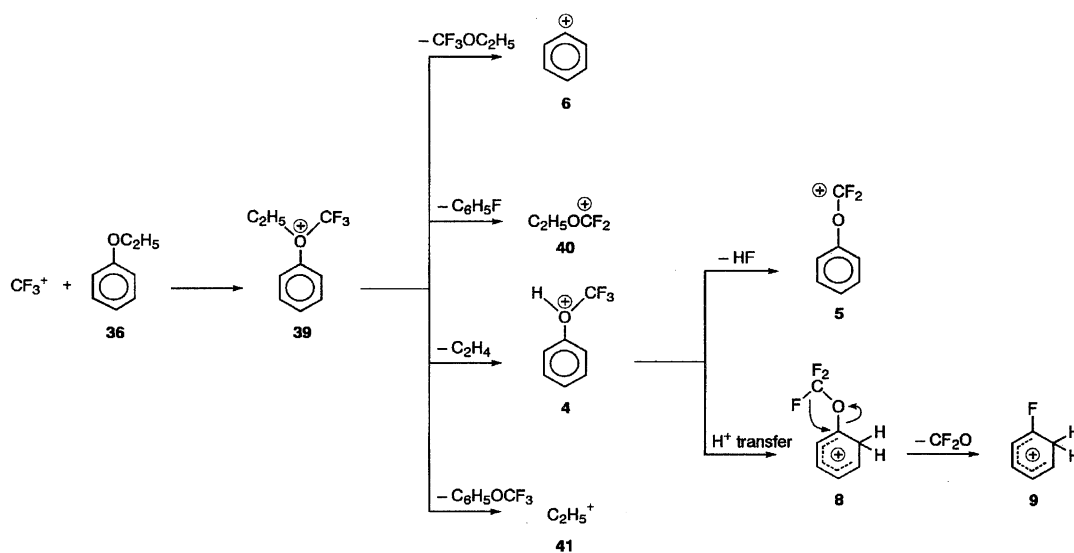
$\text{C}_6\text{H}_6\text{O}^{++}$ isomers, 42a and 42b, have been proposed as possible $\text{C}_6\text{H}_6\text{O}^{++}$ ions.¹³⁾ The ΔH° values of processes (8f) were calculated by using reported data and a calculated ΔH° value of 42b. The observed $\text{C}_6\text{H}_6\text{O}^{++}$ ion must be phenol cation 42a because the formation of 42b is energetically inaccessible, as shown in Scheme 15.

Conclusion

The gas-phase ion-molecule reactions of CF_3^+ with mono-substituted benzenes carrying a hydroxy or alkoxy group have been studied at near-thermal energy. The branching ratios of electrophilic addition to ring and substituent, HT, and CT are summarized in Table 2. On the basis of the measurements of mass-analyzed ion kinetic energy spectra,^{14,15)}



Scheme 13.



Scheme 14.

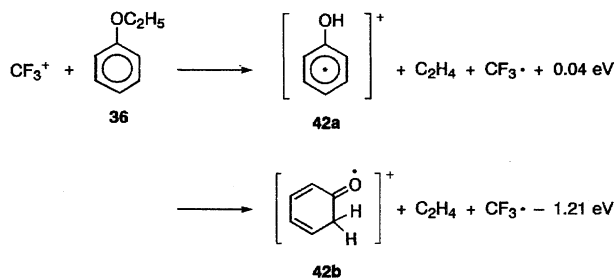
electrophilic addition of H^+ , CH_3^+ , and C_2H_5^+ to PhOH occurs dominantly on the substituent, while mixtures of ring and substituent adducts have been obtained for the reactions with CH_2Cl^+ and CHCl_2^+ . In the present study, it was found that electrophilic addition of CF_3^+ occurs exclusively on the substituent for PhCH_2OH , while both the ring and substituent addition takes place for $\text{PhCH}_2\text{CH}_2\text{OH}$, PhCH-

$(\text{OH})\text{CH}_3$, and PhOCH_3 . For the reactions with PhOH and PhOC_2H_5 , there are some ions for which it is difficult to determine whether they are produced through ring adducts or substituent ones. Therefore, there are large uncertainties of the branching ratios between the ring and substituent addition for these two reagents. In order to obtain further information on the mechanism of the electrophilic-addition/molecular-

Table 2. Reaction Mechanism of CF_3^+ with Monosubstituted Benzenes Carrying a Hydroxy or Alkoxy Group at Near-Thermal Energy

Reagent		Ionization potential/eV				Branching ratio of each reaction/%	
		Ref. 9	MNDO	AM1	PM3	Electrophilic addition	Charge transfer
$\text{C}_6\text{H}_5\text{OH}$	This work	8.47				$0-37.1 \pm 1.8$ (R), $^{a)}$ $58.1 \pm 3.0-95.2 \pm 4.8$ (S) ^{b)}	4.8 ± 1.3
$\text{C}_6\text{H}_5\text{CH}_2\text{OH}$	This work	8.50				100(S)	
$\text{C}_6\text{H}_5\text{CH}_2\text{CH}_2\text{OH}$	This work		9.32	9.39	9.46	25.2 ± 2.5 (R), 74.8 ± 3.6 (S)	
$\text{C}_6\text{H}_5\text{CH}(\text{OH})\text{CH}_3$	This work		9.33	9.47	9.58	36.0 ± 2.2 (R), 64.0 ± 2.2 (S)	
$\text{C}_6\text{H}_5\text{OCH}_3$	Ref. 2	8.82				35.7 ± 4.3 (R), 49.9 ± 8.1 (S)	14.4 ± 1.8
$\text{C}_6\text{H}_5\text{OC}_2\text{H}_5$	This work	8.13				$0-70.9 \pm 4.6$ (R), $13.7 \pm 2.0-84.6 \pm 6.6$ (S)	15.4 ± 1.4

a) Addition to benzene ring. b) Addition to substituent.



Scheme 15.

elimination pathways, an isotopic study and ab initio calculations of energy barriers in each pathway will be required.

As minor product channels, CT was found for PhOH, PhOCH₃, and PhOC₂H₅. The lack of CT for PhCH₂CH₂OH and PhCH(OH)CH₃ could be explained by calculated IP values which were higher than the recombination energy of CF_3^+ (≤ 8.90 eV). Although the IP value of PhCH₂OH is lower than the recombination energy of CF_3^+ , no CT channel could be found.

The authors are grateful to Dr. Takaaki Sonoda and Mr. Hiroki Ujita in our institute for their helpful discussions. This work was supported by a Grant-in-Aid for Scientific Research No. 06453026 from the Ministry of Education, Science, Sports and Culture, the Iwatani Naoji Memorial Foundation, and the Showa Shell Sekiyu Foundation for Promotion of Environmental Research.

References

- 1) M. Tsuji, M. Aizawa, and Y. Nishimura, *Chem. Lett.*, **1995**, 211.
- 2) M. Tsuji, M. Aizawa, and Y. Nishimura, *J. Mass Spectrom. Soc. Jpn.*, **43**, 109 (1995).
- 3) M. Tsuji, M. Aizawa, H. Ujita, and Y. Nishimura, *Bull. Chem. Soc. Jpn.*, **68**, 2385 (1995).
- 4) M. Tsuji, M. Aizawa, and Y. Nishimura, *Bull. Chem. Soc. Jpn.*, in press.
- 5) J. B. Anderson, in "Molecular Beams and Low Density Gas Dynamics," ed by P. P. Wegener, Dekker, New York (1974), Vol. 4, p. 1.
- 6) F. Grandinetti, G. Occhiucci, M. E. Crestoni, S. Fornarini, and M. Speranza, *Int. J. Mass Spectrom. Ion Processes*, **127**, 123 (1993).
- 7) F. Grandinetti, M. E. Crestoni, S. Fornarini, and M. Speranza, *Int. J. Mass Spectrom. Ion Processes*, **130**, 207 (1994).
- 8) H. M. Rosenstock, K. Draxl, G. W. Steiner, and J. T. Herron, *J. Phys. Chem. Ref. Data*, **6**, Suppl. 1 (1977).
- 9) S. G. Lias, J. E. Bartmess, J. F. Liebman, J. L. Holmes, R. D. Levin, and W. G. Mallard, *J. Phys. Chem. Ref. Data*, **17**, Suppl. 1 (1988).
- 10) J. R. Eyler, P. Ausloos, and S. G. Lias, *J. Am. Chem. Soc.*, **96**, 3673 (1974); P. Ausloos, S. G. Lias, and J. R. Eyler, *Int. J. Mass Spectrom. Ion Phys.*, **18**, 261 (1975).
- 11) G. Weddle and R. C. Dunbar, *Int. J. Mass Spectrom. Ion Processes*, **134**, 73 (1994).
- 12) A. Cornu and R. Massot, "Compilation of Mass Spectral Data," Heiden & Son Ltd., London (1966).
- 13) H. Buzikiewicz, C. Djerassi, and D. H. Williams, "Mass Spectrometry of Organic Compounds," Holden-Day Inc., San Francisco (1967).
- 14) K. V. Wood, D. J. Burinsky, D. Cameron, and R. G. Cooks, *J. Org. Chem.*, **48**, 5236 (1983).
- 15) D. J. Burinsky and J. E. Campana, *Org. Mass Spectrom.*, **23**, 613 (1988).